DOI: 10.1002/ejic.200500541

Crystal Structures, EPR Spectra, and Magnetic Properties of a Series of Ionic Multi-Component Complexes $[(TBPDA)_2{\cdot}(C_{60}^{\cdot-}){\cdot}(D^+)]$ (D = Cp^*_2Cr, Cp^*_2Co, TDAE)

Dmitri V. Konarev,*[a,b] Andrey Yu. Kovalevsky,[c] Salavat S. Khasanov,[a,d] Gunzi Saito,*[a] Akihiro Otsuka,[a,e] and Rimma N. Lyubovskaya[b]

Keywords: Crystal engineering / EPR spectroscopy / Fullerenes / IR spectroscopy / Magnetic properties / Metallocenes

New ionic multi-component complexes $[(TBPDA)_2{\cdot}(C_{60}^{\cdot-}){\cdot}(D^+)]$ [TBPDA = *N*,*N*,*N*′,*N*′-tetrabenzyl-*p*-phenylenediamine; D = decamethylchromocene (Cp^*_2Cr, **1**) and decamethylcobaltocene (Cp^*_2Co, **2**)] were obtained additionally to previously characterized $[(TBPDA)_2{\cdot}(C_{60}^{\cdot-}){\cdot}(TDAE^{\cdot+})]$ [TDAE = tetrakis(dimethylamino)ethylene, **3**]. The presence of D^+, $C_{60}^{\cdot-}$, and neutral TBPDA in **1**–**3** was proved by the IR and UV/Visible/NIR spectra. D^+ and $C_{60}^{\cdot-}$ form loose layers in **1** and **3** and are spatially separated by bulky TBPDA molecules. The $C_{60}^{\cdot-}$ radical anions alternate in the layer with the phenylene groups of TBPDA to form π-π stacking, whereas disordered $Cp^*_2Cr^+$ cations are isolated in the voids formed by eight benzyl groups of TBPDA. The EPR spectra of the complexes show single Lorentzian lines with g = 2.2526 and ΔH = 215 mT (**1**), g = 1.9999 and ΔH = 6.7 mT (**2**), and g = 2.0009 and ΔH = 2.93 mT (**3**) at room temperature. The EPR signal of **2** was attributed to $C_{60}^{\cdot-}$ ($Cp^*_2Co^+$ is diamagnetic) and those in **1** and **3** to resonating signals between $C_{60}^{\cdot-}$ (g = 1.9996–2.0000) and $Cp^*_2Cr^+$ [an asymmetric EPR signal with $g_\perp$ = 4.02(1) and $g_\parallel$ = 2.001(1)] (**1**) or $TDAE^{\cdot+}$ (g = 2.0035; **3**) due to indirect coupling. The EPR signals from **2** and **3** are split into two components below 50 and 60 K, respectively, which shift in the opposite directions (to lower and higher fields) with decreasing temperature. The magnetic moments of **1**–**3** decrease below 50–100 K. Both effects are associated with the formation of field-induced short-range antiferromagnetically ordered clusters. It is shown that the D^+ cations do not noticeably affect this interaction. Most probably, it is realized mainly between $C_{60}^{\cdot-}$ spins within the layer and is mediated by the phenylene groups of TBPDA.

Introduction

Fullerenes, as acceptors, form molecular and ionic complexes with different donor molecules.[1–3] Ionic complexes are interesting due to their magnetic properties,[4] the reversible formation of diamagnetic single-bonded $(C_{60}^-)_2$ dimers,[5–8] and other types of negatively charged σ-bonded structures.[9] However, only a limited number of organic and organometallic donors can ionize fullerenes in the solid state. These include metallocenes [decamethylnickelocene, Cp^*_2Ni;[10] decamethylchromocene, Cp^*_2Cr;[6,7] decamethylcobaltocene, Cp^*_2Co;[11,12] cobaltocene, Cp_2Co;[7,13] bis(benzene)chromium, $Cr(C_6H_6)_2$,[7,14] and its substituted analogs;[8,15,16] $Fe^ICp(C_6Me_6)$[17]], unsaturated amines [tetrakis(dimethylamino)ethylene, TDAE, and related compounds[4,18]], and some metalloporphyrins.[19,20] We have developed a multi-component approach to modify ionic complexes of fullerenes, in which a neutral D_1 molecule is introduced into an ionic complex to produce a new compound with two donor counterparts: $(D_1){\cdot}(D_2^{\cdot+}){\cdot}(\text{fullerene}^{\cdot-})$.[21–24] In such a complex, D_1 forms a supramolecular packing pattern, whereas D_2 is a strong donor of a small size relative to D_1 that is potentially able to ionize the fullerene moiety. D_1 defines not only the complex structure but in some cases affects the electronic state of the fullerenes. In the series of complexes $[Co^{II}TPP{\cdot}(D_2^+){\cdot}(C_{60}^-){\cdot}\text{solvent}]$ [$Co^{II}TPP$ = cobalt(II) tetraphenylporphyrin; D_2 = $Cr(C_6H_6)_2$[21] or TDAE[22]] $Co^{II}TPP$ forms unusual diamagnetic σ-bonded ($Co^{II}TPP{\cdot}\text{fullerene}^-$) anions, whereas in $[CTV{\cdot}(Cs^+)_2{\cdot}(C_{60(70)}^-)_2{\cdot}(DMF)_x]$ (CTV = cyclotriveratrylene; DMF = *N*,*N*′-dimethylformamide; x = 5–7) we observed the formation of single-bonded $(C_{60}^-)_2$ and $(C_{70}^-)_2$

[a] Division of Chemistry, Graduate School of Science, Kyoto University,
Sakyo-ku, Kyoto 606-8502, Japan
Fax: +81-75-753-4035
E-mail: saito@kuchem.kyoto-u.ac.jp
[b] Institute of Problems of Chemical Physics RAS,
Chernogolovka, Moscow region 142432, Russia
Fax: +7-096-5155420
E-mail: konarev@icp.ac.ru
[c] State University of New York at Buffalo,
Buffalo, New York, 14260, USA
E-mail: bioayk@langate.gsu.edu
[d] Institute of Solid State Physics RAS,
Chernogolovka, Moscow region, 142432, Russia
E-mail: khasanov@issp.ac.ru
[e] Research Center for Low Temperature and Materials Sciences, Kyoto University,
Sakyo-ku, Kyoto 606-8502, Japan
Supporting information for this article is available on the WWW under http://www.eurjic.org or from the author.

dimers[23,24] and in [(TBPDA)$_2$·($C_{60}^{\cdot-}$)·($TDAE^{\cdot+}$)] (Figure 1) a short-range antiferromagnetic interaction of the spins was found.[22] In the present work we have studied the incorporation of cations other than $TDAE^{\cdot+}$ into the (TBPDA)$_2$·C_{60} framework. We used two strong donors − Cp^*_2Cr and Cp^*_2Co (Figure 1) − that ionize C_{60} in the solid state[6,7,11,12] and whose cations are comparable in size to the $TDAE^{\cdot+}$ ones but have different spin states ($Cp^*_2Cr^+$: S = 3/2; $Cp^*_2Co^+$: S = 0) relative to that of $TDAE^{\cdot+}$ (S = 1/2). Thus, we can study how cations with different spin states and shapes ($Cp^*_2Cr^+$, $Cp^*_2Co^+$, and $TDAE^{\cdot+}$) can affect the EPR spectra and the magnetic and structural properties of a series of multi-component complexes [(TBPDA)$_2$·($C_{60}^{\cdot-}$)·(D^+)].

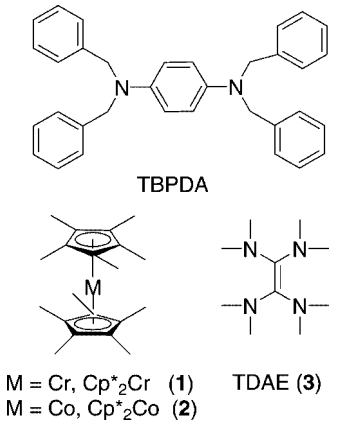

Figure 1. Molecular structures of the components used to prepare **1**–**3**.

The crystal structure of [(TBPDA)$_2$·($C_{60}^{\cdot-}$)·(Cp^*Cr^+)] (**1**) is studied for the first time; the IR and UV/Visible/NIR spectra and the EPR and magnetic susceptibility data down to liquid helium temperatures are presented for **1** and [(TBPDA)$_2$·($C_{60}^{\cdot-}$)·(Cp^*Co^+)] (**2**). These data are compared with those for previously described [(TBPDA)$_2$·($C_{60}^{\cdot-}$)·($TDAE^+$)] (**3**).[22]

Results and Discussion

Synthesis

Complexes **1** and **2** were obtained by a diffusion method in which C_{60}, Cp^*_2M, and an excess of TBPDA dissolved in a mixture of C_6H_6 and C_6H_5CN were precipitated with hexane. Previously, [(TBPDA)$_2$·C_{60}·TDAE] (**3**) was synthesized by the same procedure.[22] The use of smaller Cp_2Co or $Cr(C_6H_6)_2$ molecules under similar conditions did not afford multi-component complexes. Therefore, the size of the D_2 component is important for the stabilization of the [(TBPDA)$_2$·($C_{60}^{\cdot-}$)·(D_2^+)] complexes.

IR and UV/Visible/NIR Spectra

The IR spectra of **1** and **2** in a KBr matrix are a superposition of the spectra of C_{60}, Cp^*_2M, and TBPDA (see Supporting Information). Neutral C_{60} has absorption bands at 527, 577, 1182, and 1429 cm^{-1} [F_{1u}(1–4) modes, respectively]. The F_{1u}(1) and -(2) modes retain their positions (at 526–527 and 575 cm^{-1}), whereas the F_{1u}(4) mode, which is the most sensitive to charge transfer to the C_{60} molecule,[25] is shifted to 1388 cm^{-1} in the spectra of **1** and **2**. The integral intensity of the F_{1u}(2) mode also essentially increases relative to that of the F_{1u}(1) mode. Such changes are characteristic of $C_{60}^{\cdot-}$.[25] The formation of $C_{60}^{\cdot-}$ is justified by the appearance of additional bands in the UV/Visible/NIR spectra of **1** and **2** at 10.75–10.77 × 10^3 and 9.20 × 10^3 cm^{-1}.

Cp^*_2Cr has one band in the IR spectrum that is sensitive to charge transfer and is shifted from 418 to 437 cm^{-1} due to the transition from a neutral to a cationic form in **1** as well as in ($Cp^*_2Cr^+$)·(PF_6^-)[26] and ($Cp^*_2Cr^+$)·($C_{60}^{\cdot-}$)·($C_6H_4Cl_2$)$_2$.[6,7] Similarly, the band of Cp^*_2Co in the IR spectrum is shifted from 429 to 442, 448, and 445 cm^{-1} in **2**, ($Cp^*_2Co^+$)·(PF_6^-),[26] and [($Cp^*_2Co^+$)$_2$·(C_{60}^{2-})·($C_6H_4Cl_2$, C_6H_5CN)$_2$],[12] respectively. The absorption bands of TBPDA in the IR spectrum are shifted by up to 10 cm^{-1} in **1** and **2** relative to those in the spectrum of neutral TBPDA·(C_{60})$_2$.[27] This is probably associated with the different geometry of TBPDA in **1**, **2**, and TBPDA·(C_{60})$_2$. The absence of additional absorption bands in the IR and UV/Visible/NIR spectra of **1** and **2**, which must accompany the dimerization or polymerization of $C_{60}^{\cdot-}$,[28] indicates their monomeric nature at room temperature (room temp.). Complex **3**[22] has IR and UV/Visible/NIR spectra similar to those of **1** and **2**.

Crystal Structures

Complex **1** crystallizes in a tetragonal system in the $I\bar{4}$ space group and has a structure similar to that of [(TBPDA)$_2$·C_{60}·TDAE] (**3**)[22] (see Figures 2 and 3). $C_{60}^{\cdot-}$ and $Cp^*_2Cr^+$ (**1**) or $TDAE^{\cdot+}$ (**3**) occupy positions with $\bar{4}$ or 4/m symmetry and are statistically disordered in both structures as they lie on a symmetry position higher than their own symmetry. Complex **1** has a more complicated disorder pattern than **3**. A fourfold inversion axis passes through the midpoints of oppositely located 6-6 bonds of $C_{60}^{\cdot-}$ and the central C=C bond of $TDAE^{\cdot+}$ in **3** and coincides with the twofold symmetry axes of these ions. The rotation of both ions by 90° about a fourfold axis generates two orientations with equal occupancies.[22] In contrast to **3**, the fourfold inversion axis in **1** passes through the midpoints of oppositely located 6–5 bonds of C_{60} and the Cr atom of $Cp^*_2Cr^+$ to form an angle of about 85° with a fivefold symmetry axis of $Cp^*_2Cr^+$ (as shown in Figure 4). In this case, the symmetry operation generates four orientations of the $C_{60}^{\cdot-}$ and $Cp^*_2Cr^+$ ions with equal occupancies. The ordered TBPDA molecules occupy positions with 2/m symmetry.

The unit-cell parameters a and b (see Experimental Section) are larger by 0.35 Å in **1** than in **3**, whereas the parameter c is smaller by 0.32 Å. The unit-cell volume of **1** is increased by about 180 Å^3 relative to that of **3**, thus indicat-

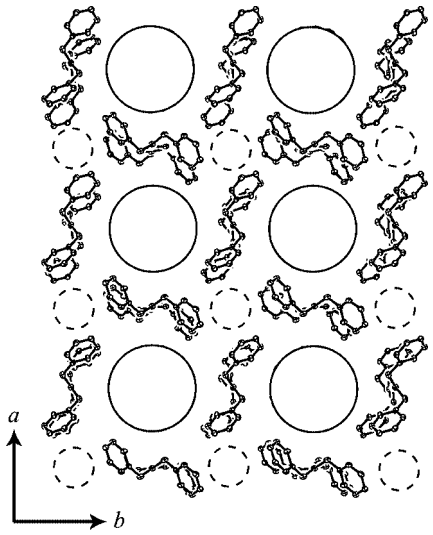

Figure 2. General view of the crystal structures of **1** and **3** on the *ab* plane. The positions of disordered $C_{60}^{\cdot-}$ radical anions are shown by large circles and those of the cations ($Cp^*_2Cr^+$ and $TDAE^{\cdot+}$) are shown by smaller dashed circles.

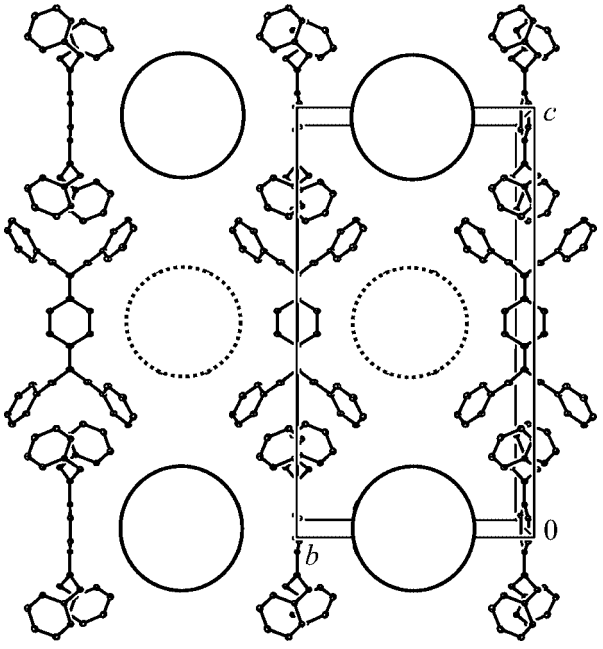

Figure 3. General view of the crystal structures of **1** and **3** on the *bc* plane. The positions of disordered $C_{60}^{\cdot-}$ radical anions are shown by large circles and those of the cations ($Cp^*_2Cr^+$ and $TDAE^{\cdot+}$) are shown by smaller dashed circles.

ing that $Cp^*_2Cr^+$ is slightly larger than $TDAE^{\cdot+}$. $C_{60}^{\cdot-}$, $Cp^*_2Cr^+$ ($TDAE^{\cdot+}$), and TBPDA form square loose layers in **1** and **3** parallel to the *ab* plane (Figure 2). The $C_{60}^{\cdot-}$ radical anions are separated from each other [the shortest center-to-center distance between adjacent fullerenes in the layer is 13.973(2) Å in **1** and 13.626(2) in **3**] and alternate with the central phenylene (-C_6H_4-) groups of TBPDA along the *a* and *b* directions (Figure 2). Consequently, each $C_{60}^{\cdot-}$ forms van der Waals contacts with four phenylene groups of the adjacent TBPDA molecules. The hexagons of

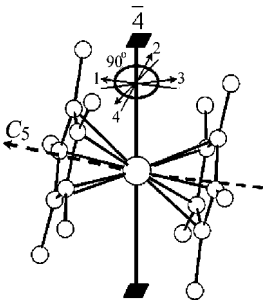

Figure 4. Disorder of the $Cp^*_2Cr^+$ cations. A fourfold inversion axis (solid line) and a fivefold symmetry axis of $Cp^*_2Cr^+$ (dashed line) are shown. Both axes form an angle of ca. 85°. Four positions of $Cp^*_2Cr^+$ with equal occupancies obtained by its rotation by 90° about a fourfold axis are marked by the numbers from 1 to 4.

$C_{60}^{\cdot-}$ and the phenylene groups of TBPDA are nearly parallel in **3** (the corresponding dihedral angle is only 5°), thus indicating the presence of π-π interactions. The C(TBPDA)···$C(C_{60}^{\cdot-})$ contacts lie in the range 3.43–3.68 Å (the sum of the van der Waals radii of two sp^2 carbon atoms is 3.42 Å[29]). Large disorder in **1** does not allow the estimation of the C···C contacts and angles. Nevertheless, the C···C contacts should be slightly larger than those in **3** due to the larger unit-cell parameters *a* and *b*.

Each $Cp^*_2Cr^+$ moiety is located within the layer in the cavities formed by eight benzyl groups of TBPDA (Figure 2). All C(TBPDA)···C($Cp^*_2Cr^+$ or $TDAE^{\cdot+}$) contacts are large (>3.70 Å) to prevent π-π interactions between the Cp* rings and TBPDA fragments. Therefore, the $Cp^*_2Cr^+$ cations are separated from each other. The interlayer space is filled with the benzyl groups of TBPDA (Figure 3). The ordered TBPDA molecules retain pristine geometry, thus showing their neutral state in the complex. Only the torsion angles of the benzyl groups of the TBPDA molecule in **1** are smaller (73°) than those in neutral TBPDA (85–87°).[30] Such changes are probably caused by packing forces.

A schematic view of the crystal structures of **1** and **3** along the *a* direction is shown in Figure 3. The chains of alternating $C_{60}^{\cdot-}$ and D^+ ions can be seen along the *c* direction. These chains are separated from the neighboring ones by bulky TBPDA molecules. The distances between the $C_{60}^{\cdot-}$ and D^+ ions in the chains are rather large [all intermolecular C(C_{60})···C(D^+) contacts are longer than 5 Å]. Thus, **1** and **3** are dilute systems in which the $C_{60}^{\cdot-}$ and D^+ ions are separated in three directions by the TBPDA molecules. Nevertheless, the $C_{60}^{\cdot-}$ radical anions alternate and form π-π interactions with the phenylene groups of TBPDA, which can mediate magnetic coupling between $C_{60}^{\cdot-}$ spins within the layer. The TBPDA molecules can probably also mediate weak coupling between spins localized on $C_{60}^{\cdot-}$ and D^+.

Magnetic Properties

The magnetic properties of polycrystalline **1**, **2**, and **3**[33] sealed in quartz tubes under 10^{-5} Torr vacuum were studied by EPR (Table 1, Figures 5 and 6) and SQUID (Figure 7)

techniques from room temp. down to liquid helium temperatures.

Table 1. EPR parameters of **1**–**3**.

Complex	290 K		4 K	
	g factor	ΔH [mT]	*g* factor	ΔH [mT]
$[(TBPDA)_2{\cdot}C_{60}{\cdot}Cp^*_2Cr]$ (**1**)	1.9999	6.7	1.9985	0.42
			1.9950	0.51
$[(TBPDA)_2{\cdot}C_{60}{\cdot}Cp^*_2Co]$ (**2**)	2.2526	215	2.7563	168
$[(TBPDA)_2{\cdot}C_{60}{\cdot}TDAE]$ (**3**)[22]	2.0009	2.93	2.0063	0.76
			1.9966	0.21

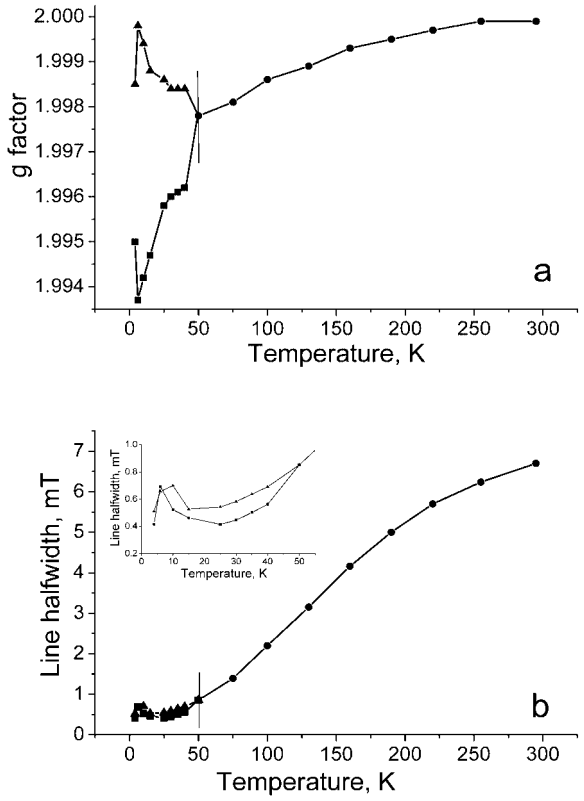

Figure 5. Temperature dependence of the *g*-factor (a) and line halfwidth (b) for $[(TBPDA)_2{\cdot}C_{60}{\cdot}Cp^*_2Co]$ (**2**) in the 4–295 K range.

Complex **2** shows a broad Lorentzian line with g = 1.9999 and line halfwidth (ΔH) of 6.7 mT (Figure 5). This signal is characteristic of $C_{60}^{\cdot-}$, which has a *g*-factor in the range 1.9996–2.0000 and ΔH of 3–5 mT at room temp.[2,3] Diamagnetic and EPR silent $Cp^*_2Co^+$ makes no contribution to the EPR spectrum of **2**.

The EPR signal of **3** has a larger *g*-factor of 2.0009 and a narrower line (ΔH = 2.93 mT).[22] $TDAE{\cdot}C_{60}$ has a similar EPR signal (g = 2.0003 and ΔH = 2.2 mT at room temp.[31]). Both signals can be attributed to resonating ones between $C_{60}^{\cdot-}$ and $TDAE^{\cdot+}$ ion-radicals due to an intermediate *g*-factor value ($C_{60}^{\cdot-}$ has a *g*-factor of 1.9996–2.0000 and $TDAE^{\cdot+}$ of 2.0035[32]). The resonating signal is characteristic of exchange coupling between $TDAE^{\cdot+}$ and $C_{60}^{\cdot-}$ ion-radicals. This coupling in $TDAE{\cdot}C_{60}$ can be realized directly between both ion-radicals due to short C···C contacts (3.401–3.482 Å[33]) and the overlapping of their π-orbitals.

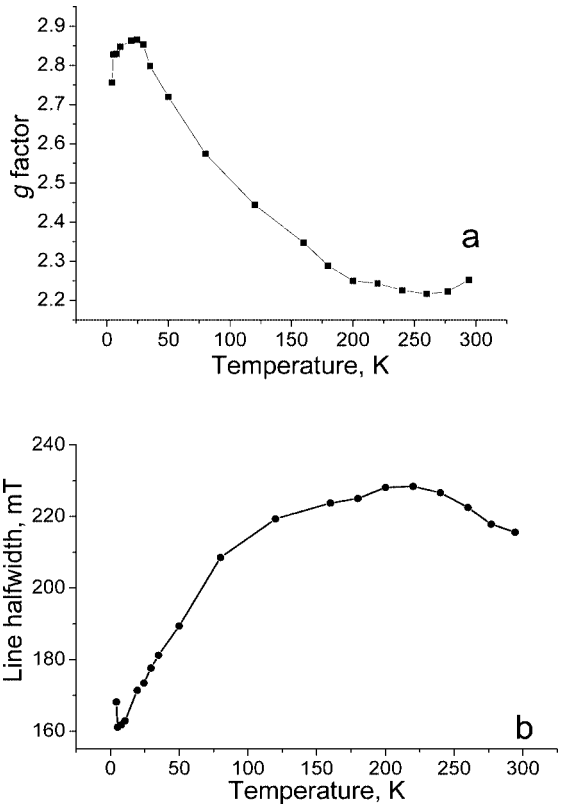

Figure 6. Temperature dependence of the *g*-factor (a) and line halfwidth (b) for $[(TBPDA)_2{\cdot}C_{60}{\cdot}Cp^*_2Cr]$ (**1**) in the 4–295 K range.

The distances between ion-radicals in **3** are large and in this case we can suppose only indirect coupling (for example, through the TBPDA molecules). Indirect coupling through nonmagnetic ligands has previously been observed even in clusters.[34]

The EPR spectrum of **1** contains a single Lorentzian line with g = 2.2526 and ΔH = 215.6 mT at room temp. (Figure 6). A similar EPR signal has been observed for a high-temperature monomeric phase of $[Cp^*_2Cr{\cdot}C_{60}{\cdot}(C_6H_4Cl_2)_2]$ (g = 2.2210 and $\Delta H \approx$ 100 mT at 320 K[24]). The observed *g*-factors are intermediate between those of $C_{60}^{\cdot-}$ and Cp^*_2Cr {an asymmetric EPR signal with $g_\perp$ = 4.02(1) and $g_\parallel$ = 2.001(1)[26]}, thus implying a resonating signal between these ions. Exchange coupling between the $Cp^*_2Cr^+$ and $C_{60}^{\cdot-}$ ions can be realized directly in $[Cp^*_2Cr{\cdot}C_{60}{\cdot}(C_6H_4Cl_2)_2]$ as the shortest C···C distance is 3.049(6) Å[6] and only indirectly in **1** due to the large distances between the ions, similar to **3**.

The EPR signal of **2** essentially narrows with decreasing temperature and the *g*-factor shifts monotonically to 1.9978 at 50 K (Figure 5). A similar behavior of ΔH has been observed for **3** and other solid ionic complexes of C_{60}.[2] The EPR signal becomes asymmetric below 50 K and splits into two components (see Supporting Information). These components shift in the opposite directions (to higher and lower magnetic fields) with decreasing temperature (g = 1.9985 and 1.9950 at 4 K, Figure 5a). The shifts are accompanied by a small broadening of both components (Figure 5b). The

magnetic moment of **2** (μ_{eff} = 1.65 μ_B at 300 K) is nearly temperature independent down to around 100 K and begins to decrease below this temperature (Figure 7b). Both effects in SQUID and EPR originate from the antiferromagnetic interaction of spins. Such a behavior can be attributed to the formation of a field-induced short-range antiferromagnetically ordered cluster.[35,36] The behavior of **3** is very similar. The temperatures of the splitting of the EPR signal and the decrease of the magnetic moment are 60 and about 80 K, respectively (Figure 7c).[22]

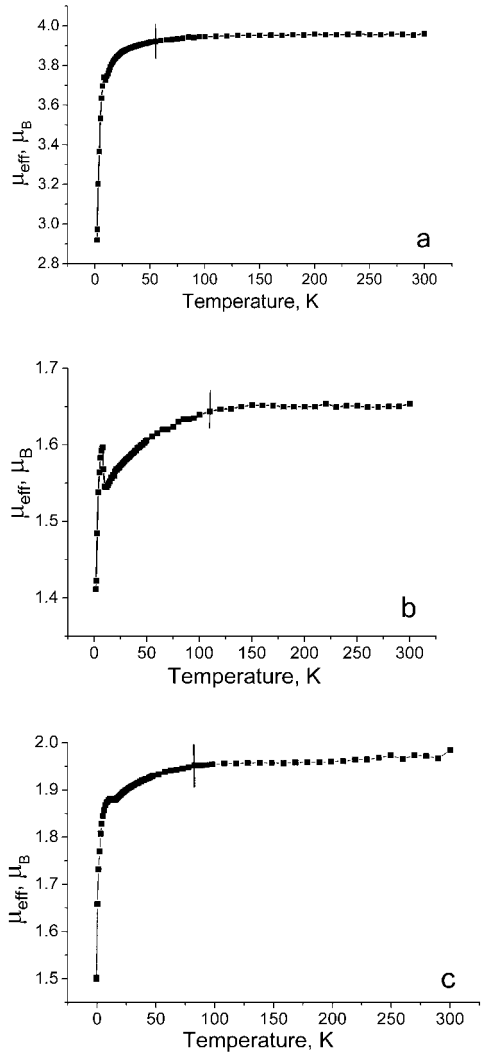

Figure 7. Temperature dependence of the magnetic moments of **1** (a), **2** (b), and **3** (c) in the 1.9–300 K range. Vertical bars show the temperature for a decrease of the magnetic moment.

The EPR signal of **1** shifts to larger *g*-factors with decreasing temperature (g = 2.7563 at 4 K, Figure 6a), whereas ΔH remains very broad in the whole temperature range (approx. 160–230 mT; Figure 6, b). The magnetic moment of **1** (μ_{eff} = 3.96 μ_B at 300 K) indicates a contribution from $Cp^*_2Cr^+$ (S = 3/2) and $C_{60}^{\cdot-}$ (S = 1/2) (μ_{eff} = 4.27 μ_B for a system of noninteracting S = 3/2 and 1/2 spins). Ionic $[Cp^*_2Cr{\cdot}C_{60}{\cdot}(C_6H_4Cl_2)_2]$[7] and $[Cr^{III}TPP{\cdot}C_{60}{\cdot}(THF)_3]$ [Cr^{III}TPP = tetraphenylporphyrinatochromium(III)][20] have similar magnetic moments equal to 4.20 μ_B. The magnetic moment of **1** is temperature independent down to around 50 K and decreases below this temperature due to the antiferromagnetic interaction of spins (Figure 7, a). However, the EPR signal of **1** is unsplit down to 4 K, probably due to a very large ΔH value.

An antiferromagnetic character of interaction of spins in **1**–**3** was justified by SQUID measurements. The complexes show small negative Weiss constants of –0.7 K for **1**, –1.8 K for **2**, and –2.3 K for **3**.

Conclusion

Two new ionic multi-component complexes $[(TBPDA)_2{\cdot}(C_{60}^{\cdot-}){\cdot}(D^+)]$ containing decamethylchromocene (Cp^*_2Cr, **1**) and decamethylcobaltocene (Cp^*_2Co, **2**) have been obtained. Together with previously characterized $[(TBPDA)_2{\cdot}(C_{60}^{\cdot-}){\cdot}(TDAE^{\cdot+})]$ (**3**), they form a series of multi-component complexes with cations of different shape and spin state. The optical absorption spectra of **1**–**3** in the IR and UV/Visible/NIR ranges prove the presence of D^+, $C_{60}^{\cdot-}$, and neutral TBPDA. The D^+ and $C_{60}^{\cdot-}$ ions in the crystal structures of **1** and **3** form loose layers that are spatially separated by the bulky TBPDA molecules. As this takes place, the $C_{60}^{\cdot-}$ radical anions alternate with the phenylene groups of TBPDA to form π-π stacking interactions with them, whereas the D^+ cations are spatially and magnetically isolated in the voids formed by eight benzyl groups of TBPDA. The complexes show single Lorentzian EPR lines with g = 1.9999 and ΔH = 6.7 mT (**2**), g = 2.0009 and ΔH = 2.93 mT (**3**), and g = 2.2526 and ΔH = 215 mT (**1**) at room temp. Two-component ionic complexes of C_{60}, namely $TDAE{\cdot}C_{60}$[31] and $[Cp^*_2Cr{\cdot}C_{60}{\cdot}(C_6H_4Cl_2)_2]$[24] have EPR signals similar to those of **3** and **1**. The EPR signal in **2** was attributed to $C_{60}^{\cdot-}$ as $Cp^*_2Co^+$ is diamagnetic and therefore EPR silent. The EPR signals in **1** and **3** and in corresponding two-component complexes were assigned to resonating signals between $C_{60}^{\cdot-}$ and D^+ ($Cp^*_2Cr^+$ or $TDAE^{\cdot+}$). In two-component complexes this is a result of direct exchange coupling between $C_{60}^{\cdot-}$ and D^+, which is possible due to short intermolecular contacts between them and the overlapping of their π-orbitals. Complexes **1** and **3** are dilute systems with large spatial separation between the $C_{60}^{\cdot-}$ and D^+ ions. In this case only indirect coupling can be supposed through the TBPDA molecules. Below 60 K (**3**) and 50 K (**2**), the EPR signals are split into two components that shift in opposite directions to lower and higher fields. The magnetic moments of **1**–**3** also decrease below 50–100 K. These phenomena can be explained by the formation of field-induced short-range antiferromagnetically ordered clusters. The substitution of paramagnetic $Cp^*_2Cr^+$ and $TDAE^{\cdot+}$ by diamagnetic $Cp^*_2Co^+$ does not noticeably affect the antiferromagnetic interaction of the spins in **1**–**3**. In accordance with X-ray diffraction data, this interaction is realized mainly between $C_{60}^{\cdot-}$ spins within the layer through the phenylene groups of TBPDA as the D^+ cations are surrounded by benzyl groups of TBPDA and are not involved in this interaction. Nevertheless, the TBPDA mole-

cules probably mediate weak exchange coupling between the $C_{60}^{\cdot-}$ and D^+ spins seen by EPR. The large distances between $C_{60}^{\cdot-}$ and D^+ in **1**–**3** and the mediation of magnetic coupling through the diamagnetic TBPDA molecules are reasons for the relatively weak magnetic interaction of spins with Weiss constants from –0.7 to –2.3 K.

Experimental Section

General: Decamethylchromocene (Cp^*_2Cr) and decamethylcobaltocene (Cp^*_2Co) were purchased from Strem Chemicals, *N*,*N*,*N*′,*N*′-Tetrabenzyl-*p*-phenylenediamine (TBPDA) was purchased from Lancaster and C_{60} of 99.98% purity from MTR Ltd. Solvents were purified under argon. Benzonitrile (C_6H_5CN) was distilled from Na under reduced pressure; benzene and hexane were distilled from Na/benzophenone. The solvents were degassed and stored in a glove box. Synthesis of the complexes was carried out in an MBraun 150B-G glove box with controlled atmosphere (content of H_2O and O_2 less than 1 ppm). The crystals were stored in the glove box and were sealed in 2 mm quartz tubes for EPR and SQUID measurements at 10^{-5} Torr. KBr pellets for IR and UV/Visible/NIR measurements were prepared in the glove box.

UV/Visible/NIR spectra were measured on a Shimadzu-3100 spectrometer in the 240–2600 nm range. FT-IR spectra were measured as KBr pellets with a Perkin–Elmer 1000 Series spectrometer (400–7800 cm^{-1}). A Quantum Design MPMS-XL SQUID magnetometer was used to measure static susceptibilities of **1** and **2** between 300 and 1.9 K in a 0.1 T static magnetic field. A sample holder contribution and core temperature independent diamagnetic susceptibility (χ_0) were subtracted from the experimental values. The values of Θ and χ_0 were calculated from the high-temperature range using the formula $\chi_M = C/(T - \Theta) + \chi_0$. EPR spectra were recorded from room temp. down to 4 K with a JEOL JES-TE 200 X-band ESR spectrometer equipped with a JEOL ES-CT470 cryostat.

Synthesis: Crystals of [(TBPDA)$_2$·C_{60}·Cp^*_2Cr] (**1**) and [(TBPDA)$_2$·C_{60}·Cp^*_2Co] (**2**) were obtained by slow diffusion of hexane (20 mL) into 20 mL of a C_6H_6/C_6H_5CN mixture (4:1) containing C_{60} (25 mg, 0.035 mmol), Cp^*_2M (0.037 mmol), and TBPDA (120 mg, 0.255 mmol). The starting solution was prepared by dissolving C_{60} and Cp^*_2M in 4 mL of C_6H_5CN by stirring at 60 °C for 4 h. After this 16 mL of benzene was added and TBPDA was dissolved by stirring overnight at 60 °C. The obtained solution was cooled down to room temperature and filtered. Diffusion was carried out in a glass tube of 1.8 cm diameter and 50 mL volume with a ground glass plug during one month. The solvent was decanted and the crystals were washed with hexane and dried to yield black square thick plates of complexes **1** and **2** in 60–80% yield.

[(TBPDA)$_2$·C_{60}·Cp^*_2Cr] (1980.3): calcd. C 89.80, H 4.75, Cr 2.62, N 2.83; found C 89.41, H 4.86, N 2.69.

[(TBPDA)$_2$·C_{60}·Cp^*_2Co] (1987.2): calcd. C 89.48, H 4.73; Co 2.97, N 2.82; found C 89.00, H 4.65, N 2.64.

The composition of **1** and **2** was determined from the elemental analysis, and was justified for **1** by X-ray diffraction on a single crystal. The synthesis of crystals of **3** has been described elsewhere.[22]

X-ray Crystallographic Study of 1: $C_{148}H_{94}CrN_4$, M_r = 1980.27, black square plates, tetragonal, space group $I\bar{4}$. Unit cell parameters $a = b$ = 13.9732(3), c = 24.3682(11) Å, V = 4757.9(3) Å^3, Z = 2, D_c = 1.382 g cm^{-3}, μ = 0.186 mm^{-1}, and $F(000)$ = 2068. X-ray diffraction data for **1** were collected at 90(1) K using a Bruker SMART1000 CCD diffractometer installed at a rotating anode source (Mo-K_α radiation, λ = 0.71073 Å), and equipped with an Oxford Cryosystems nitrogen gas-flow apparatus. The data were collected by the rotation method with a 0.3° frame-width (ω scan) and 10 s exposure time per frame. Four sets of data (600 frames in each set) were collected, nominally covering half of the reciprocal space. The data were integrated, scaled, sorted, and averaged using the SMART software package.[37] In total, 42648 reflections were measured up to $2\Theta_{max}$ = 59.98°, 6879 of which were independent. The structure was solved by direct methods using SHELXTL NT Version 5.10.[38] The structure was refined by full-matrix least-squares against F^2. Non-hydrogen atoms were refined in the anisotropic approximation. Positions of hydrogen atoms were calculated geometrically. Subsequently, the positions of H atoms were refined by the "riding" model with U_{iso} = 1.2 U_{eq} of the connected non-hydrogen atom or as ideal CH_3 groups with U_{iso} = 1.5 U_{eq}. The least-squares refinement on F^2 was done to $R_1[I > 2\sigma(F)]$ = 0.0885 for 5626 observed reflections with $F > 2\sigma(F)$, wR_2 = 0.2358 and R_1 = 0.1053 for all 6879 observed reflections with 482 parameters and 7956 restraints; final GoF = 1.078.

CCDC-275769 contains the supplementary crystallographic data for compound **1**. These data can be obtained free of charge from The Cambridge Crystallographic Data Center via www.ccdc.cam.ac.uk/data_request/cif.

Supporting Information (for details see the footnote on the first page of this article): IR, UV/Visible/NIR, and EPR spectroscopic data of complexes **1**–**3** (Tables S1 and S2 and Figures S1–S4).

Acknowledgments

The work was partly supported by a Grant-in-Aid for Scientific Research from the Ministry of Education, Culture, Sports, Science and Technology, Japan (152005019, 21st Century COE, and Elements Science 12CE2005) and the RFBR grant no. 03-03-32699a.

[1] A. L. Balch, M. M. Olmstead, *Chem. Rev.* **1998**, *98*, 2123–2165.
[2] C. A. Reed, R. D. Bolskar, *Chem. Rev.* **2000**, *100*, 1075–1120.
[3] D. V. Konarev, R. N. Lyubovskaya, *Russ. Chem. Rev.* **1999**, *68*, 19–38.
[4] B. Gotschy, *Fullerene Sci. Technol.* **1996**, *4*, 677–698.
[5] A. Hönnerscheid, L. van Wüllen, M. Jansen, J. Rahmer, M. Mehring, *J. Chem. Phys.* **2001**, *115*, 7161–7165.
[6] D. V. Konarev, S. S. Khasanov, A. Otsuka, G. Saito, *J. Am. Chem. Soc.* **2002**, *124*, 8520–8521.
[7] D. V. Konarev, S. S. Khasanov, G. Saito, A. Otsuka, Y. Yoshida, R. N. Lyubovskaya, *J. Am. Chem. Soc.* **2003**, *125*, 10074–10083.
[8] S. Yu. Ketkov, G. A. Domrachev, A. M. Ob'edkov, A. Yu. Vasil'kov, L. P. Yur'eva, C. P. Mehner, *Russ. Chem. Bull.* **2004**, *53*, 2056–2059.
[9] K. Prassides, in *The Physics of Fullerene-Based and Fullerene-Related Materials* (Ed.: W. Andreoni), Kluwer Academic Publishers, The Netherlands, **2000**, pp. 175–202.
[10] W. C. Wan, X. Liu, G. M. Sweeney, W. E. Broderick, *J. Am. Chem. Soc.* **1995**, *117*, 9580–9581.
[11] P. D. W. Boyd, P. Bhyrappa, P. Paul, J. Stinchcombe, R. D. Bolskar, Y. Sun, C. A. Reed, *J. Am. Chem. Soc.* **1995**, *117*, 2907–2914.
[12] D. V. Konarev, S. S. Khasanov, G. Saito, I. I. Vorontsov, A. Otsuka, R. N. Lyubovskaya, Yu. M. Antipin, *Inorg. Chem.* **2003**, *42*, 3706–3708.
[13] A. L. Balch, J. W. Lee, B. C. Noll, M. M. Olmstead, *Recent Advances in the Chemistry and Physics of Fullerenes and Related Materials* (Eds.: K. M. Kadish, R. S. Ruoff), **1994**, vol. 24, 1231–1243.

[14] Y. Yoshida, A. Otsuka, O. O. Drozdova, K. Yakushi, G. Saito, *J. Mater. Chem.* **2003**, *13*, 252–258.
[15] W. E. Broderick, K. W. Choi, W. C. Wan, *Electrochem. Soc. Proc.* **1997**, *14*, 1102–1113.
[16] A. Hönnerscheid, L. van Wüllen, R. Dinnebier, M. Jansen, J. Rahmer, M. Mehring, *Phys. Chem. Chem. Phys.* **2004**, *6*, 2454–2460.
[17] C. Bossard, S. Rigaut, D. Astruc, M.-H. Delvill, G. Felix, A. Fevrier-Bouvier, J. Amiell, S. Fladroids, P. Delhaes, *J. Chem. Soc., Chem. Commun.* **1993**, 333–334.
[18] P.-M. Allemand, K. C. Khemani, A. Koch, F. Wudl, K. Holczer, S. Donovan, G. Grüner, J. D. Thompson, *Science* **1991**, *253*, 301–303.
[19] A. Pénicaud, J. Hsu, C. A. Reed, A. Koch, K. Khemani, P.-M. Allemand, F. Wudl, *J. Am. Chem. Soc.* **1991**, *113*, 6698–6700.
[20] J. Stinchcombe, A. Pénicaud, P. Bhyrappa, P. D. W. Boyd, C. A. Reed, *J. Am. Chem. Soc.* **1993**, *115*, 5212–5217.
[21] D. V. Konarev, S. S. Khasanov, A. Otsuka, Y. Yoshida, R. N. Lyubovskaya, G. Saito, *Chem. Eur. J.* **2003**, *9*, 3837–3848.
[22] D. V. Konarev, I. S. Neretin, G. Saito, Yu. L. Slovokhotov, A. Otsuka, R. N. Lyubovskaya, *Dalton Trans.* **2003**, 3886–3891.
[23] D. V. Konarev, S. S. Khasanov, I. I. Vorontsov, G. Saito, Yu. A. Antipin, A. Otsuka, R. N. Lyubovskaya, *Chem. Commun.* **2002**, 2548–2549.
[24] D. V. Konarev, S. S. Khasanov, G. Saito, R. N. Lyubovskaya, *Recent Research Developments in Chemistry*, vol. 2, Research Signpost, Trivandrum, Kerala, India, **2004**, 105–140.
[25] T. Picher, R. Winkler, H. Kuzmany, *Phys. Rev. B* **1994**, *49*, 15879–15889.
[26] J. L. Robbins, N. Edelstein, B. Spencer, J. C. Smart, *J. Am. Chem. Soc.* **1982**, *104*, 1882–1893.
[27] D. V. Konarev, A. Yu. Kovalevsky, A. L. Litvinov, N. V. Drichko, B. P. Tarasov, P. Coppens, R. N. Lyubovskaya, *J. Solid State Chem.* **2002**, *168*, 474–485.
[28] M. S. Dresselhaus, G. Dresselhaus, in *Fullerene Polymers and Fullerene Polymer Composites* (Eds.: P. C. Eklund, A. M. Rao), Springer-Verlag, Berlin, **1999**, pp. 1–57.
[29] R. S. Rowland, R. Taylor, *J. Phys. Chem.* **1996**, *100*, 7384–7391.
[30] C. Richert, M. Pirotta, T. Muller, *Acta Crystallogr., Sect. C* **1992**, *48*, 2233–2235.
[31] K. Tanaka, A. A. Zakhidov, K. Yoshizawa, K. Okahara, T. Yamabe, K. Yakushi, K. Kikuchi, S. Suzuku, L. Ikemoto, Y. Achiba, *Phys. Rev. B* **1993**, *47*, 7554–7559.
[32] K. Kuwata, D. H. Geske, *J. Am. Chem. Soc.* **1964**, *86*, 2101–2105.
[33] B. Narymbetov, H. Kobayashi, M. Tokumoto, A. Omerzu, D. Mihailovic, *Chem. Commun.* **1999**, 1511–1512.
[34] P. W. Anderson, *Magnetism*, N. Y. Academic, **1963**, vol. 1, p. 25.
[35] D. Arčon, R. Blinc, P. Cevk, G. Chouteau, A.-L. Barra, *Phys. Rev. B* **1997**, *56*, 10786–10788.
[36] A. L. Maneiro, L. Pasimeni, L. C. Brunel, L. A. Pardi, G. Cao, R. P. Guertin, *Solid State Commun.* **1998**, *106*, 727–732.
[37] SMART and SAINT, Area detector control and integration software, Ver. 6.01. Bruker Analytical X-ray Systems, Madison, Wisconsin, U.S.A., **1999**.
[38] SHELXTL, An integrated system for solving, refining and displaying crystal structures from diffraction data, Ver. 5.10. Bruker Analytical X-ray Systems, Madison, Wisconsin, U.S.A, **1997**.

Received: June 21, 2005
Published Online: October 12, 2005

